Venular basement membranes contain specific matrix protein low expression regions that act as exit points for emigrating neutrophils

Shijun Wang,[1] Mathieu-Benoit Voisin,[1] Karen Y. Larbi,[1] John Dangerfield,[1] Christoph Scheiermann,[1] Maxine Tran,[2] Patrick H. Maxwell,[2] Lydia Sorokin,[3] and Sussan Nourshargh[1]

[1]Cardiovascular Medicine Unit, National Heart and Lung Institute and [2]Renal Section, Division of Medicine, Faculty of Medicine, Imperial College London, Hammersmith Hospital Campus, London W12 ONN, England, UK
[3]Institute of Physiological Chemistry and Pathobiochemistry Muenster, University Waldeyerstrasse, 15 48149 Muenster, Germany

The mechanism of leukocyte migration through venular walls in vivo is largely unknown. By using immunofluorescence staining and confocal microscopy, the present study demonstrates the existence of regions within the walls of unstimulated murine cremasteric venules where expression of key vascular basement membrane (BM) constituents, laminin 10, collagen IV, and nidogen-2 (but not perlecan) are considerably lower (<60%) than the average expression detected in the same vessel. These sites were closely associated with gaps between pericytes and were preferentially used by migrating neutrophils during their passage through cytokine-stimulated venules. Although neutrophil transmigration did not alter the number/unit area of extracellular matrix protein low expression sites, the size of these regions was enlarged and their protein content was reduced in interleukin-1β–stimulated venules. These effects were entirely dependent on the presence of neutrophils and appeared to involve neutrophil-derived serine proteases. Furthermore, evidence was obtained indicating that transmigrating neutrophils carry laminins on their cell surface in vivo. Collectively, through identification of regions of low extracellular matrix protein localization that define the preferred route for transmigrating neutrophils, we have identified a plausible mechanism by which neutrophils penetrate the vascular BM without causing a gross disruption to its intricate structure.

CORRESPONDENCE
Sussan Nourshargh:
s.nourshargh@imperial.ac.uk

Abbreviations used: BM, basement membrane; LE, low expression; NE, neutrophil elastase; PF, paraformaldehyde.

The migration of leukocytes from the vascular lumen to the extravascular tissue is one of the most dramatic cellular responses observed at sites of inflammation and is a fundamental event in both innate and adaptive immunity. This response occurs via a series of complex cellular and molecular events that collectively lead to slowing down of free-flowing leukocytes in the blood stream, thus promoting a rolling response along the venular wall. This is followed by firm adhesion of leukocytes to venular endothelium and eventually migration through the vessel wall. Although substantial advances have been made in our understanding of molecular pathways that mediate leukocyte–endothelial cell interactions within the vascular lumen (1, 2), because of the complex nature of the vessel wall and the difficulties associated with modeling it in vitro (3), less is known about the molecular interactions that mediate migration of leukocytes through venular walls (4).

Venular walls have two cellular components, endothelial cells and pericytes, both of which appear to contribute to the generation of the matrix component of the vessel wall, its basement membrane (BM) (5, 6). Through formation of complex molecular organizations between adjacent cells, endothelial cells form a confluent layer within the vessel wall and provide the first barrier for emigrating leukocytes (7). There is a growing understanding of the mechanisms by which leukocytes penetrate the endothelium; recent developments in the field have led to the identification of several new

S. Wang and M.-B. Voisin contributed equally to this work.

The Journal of Experimental Medicine

molecules and adhesive interactions implicated in this process (8, 9). Specifically, in addition to PECAM-1 (CD31), the first endothelial cell junctional molecule shown to be involved in leukocyte transendothelial cell migration (10), there is now evidence for the involvement of several other molecules including ICAM-2 and members of the JAM family, CD99 and ESAM (8, 9). In addition, there is now a renewed interest in the contribution and potential mechanisms by which leukocytes may migrate through the endothelium via the transcellular route (11). Despite our increased understanding of the mechanisms associated with leukocyte transendothelial cell migration, details of the mechanisms by which leukocytes penetrate the second key barrier within venular walls, the perivascular BM, have remained ellusive.

Vascular BM is composed of a complex network of several extracellular matrix proteins. The major architectural feature of this structure is two independent protein networks formed by laminins (laminin 8 [composed of $\alpha4\beta1\gamma1$ chains] and laminin 10 [composed of $\alpha5\beta1\gamma1$ chains]) (12, 13) and collagen type IV that are largely interconnected with other components of the BM, such as nidogen-2 and perlecan (14). The perivascular BM envelops pericytes that are long cells, ~150–200 μm in length and ~10–25 μm wide, which form a discontinuous layer within the wall of all postcapillary venules (15). The venular BM acts as a significant structural support for endothelial cells, thus maintaining the venular architecture. It also serves another important function by providing a distinct and effective barrier to leukocytes and macromolecules, a barrier that has to be breached at sites of inflammation (16). The mechanism by which this occurs in vivo is, however, unknown and although in vitro studies have frequently implicated leukocyte proteases in this response (17), histological studies have consistently failed to identify defects in the structure of the BM at sites of leukocyte migration (16, 18). Neutrophils, in particular those that have undergone a transmigration step, express functionally important levels of integrins such as $\alpha_2\beta_1$ (19, 20) and $\alpha_6\beta_1$ (21–23), receptors for collagen IV and laminins, respectively. This strongly suggests that adhesive interactions between neutrophils and BM constituents may play an important role in guiding neutrophils through the venular BM. Despite these findings, in the light of the known resistance of the BM to mechanical damage and its impermeable nature, it remains unclear how neutrophils may cross this barrier without disrupting its intricate three-dimensional structure. Of relevance, Walker et al. previously reported on neutrophil migration through holes in the BM of alveolar capillaries (24), though there is no strong evidence for the existence of such regions in venular BMs.

To investigate the mechanisms by which neutrophils migrate through venular BM in more detail, in the present study we have investigated the distribution of key BM constituents in murine cremaster muscle venular walls by immunofluorescent confocal microscopy under both basal and inflammatory conditions. The findings have led to the identification of regions within the venular wall, where the expressions of certain BM constituents (e.g. laminin 10 and collagen IV) are lower than the average vascular level. Of importance, these regions are highly associated with gaps between pericytes and appear to be preferentially used by transmigrating neutrophils. Furthermore, the results provide evidence to suggest that transmigrating neutrophils induce a transient remodeling of the BM, possibly through involvement of leukocyte proteases such as neutrophil elastase (NE), that facilitates neutrophil transmigration through enlargement of the low expression (LE) regions. Collectively, by identifying vulnerable sites within the structure of the perivascular BM, the present findings provide a substantial insight into the mechanism by which neutrophils penetrate the venular wall.

RESULTS

Identification of venular matrix protein LE regions

The murine cremasteric muscle was chosen for investigating the expression profiles of vascular BM constituents because,

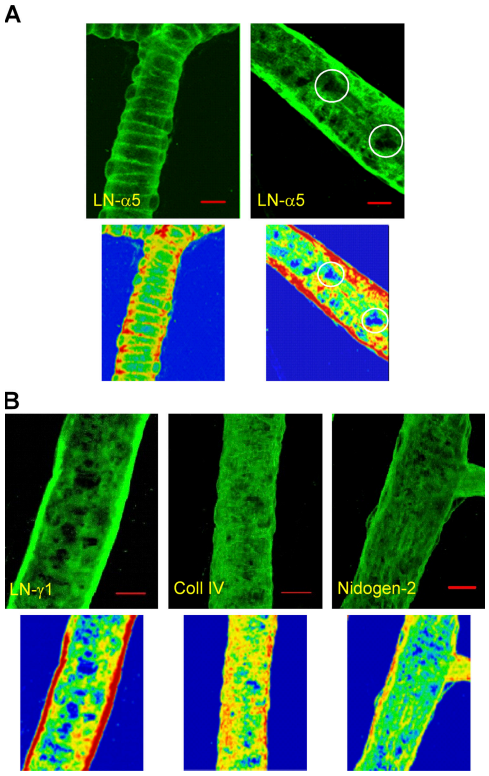

Figure 1. Expression profiles of basement membrane proteins in unstimulated cremasteric vessel walls: identification of LE regions. The figure shows representative three-dimensional images of "semi-vessels" of unstimulated cremasteric microvessels immunostained for different matrix proteins. (A) Expression of LN-α5 chain (detecting laminin 10) in an arteriole (left) and venule (right), with corresponding intensity profiles (below the images). The color coding shows low intensity sites as blue and high intensity sites as red. Representative laminin 10 LE regions in the imaged venular wall are indicated by white circles. (B) Expressions of laminin γ1 (constituent of both laminins 8 and 10), collagen IV, and nidogen-2 and their corresponding intensity profiles. Each image is representative of at least five vessels/tissue (at least $n = 4$ mice per group). Bar, 10 μm.

as a result of its thin and transparent nature, high resolution images of its microvascular bed can be obtained by immunofluorescence staining and confocal microscopy. Furthermore, it permits direct comparison of this immunofluorescent data with real-time leukocyte migration as observed by intravital microscopy.

To investigate the expression of venular BM constituents, cremaster muscles were immunostained for laminin 8 ($\alpha4\beta1\gamma1$ chains) and 10 ($\alpha5\beta1\gamma1$ chains), the principal vascular laminin isoforms (6, 12–13), in parallel with other key basement membrane components, collagen type IV (25), perlecan (26), and nidogen-2 (27), using a panel of well-characterized anti–mouse antibodies (28). Immunostaining of unstimulated whole cremasteric muscles with a rabbit anti-laminin $\alpha5$ (LN-$\alpha5$) chain polyclonal antibody (405), detecting the laminin 10 isoform, consistently indicated a discontinuous expression profile of this matrix protein in venules but not arterioles (both at 20–40 μm in diameter). Analysis of intensity profiles identified clear regions of low fluorescence intensity, and hence by extension, regions of LE of laminin 10 in venular walls (Fig. 1 A). Similar expression profile of laminin 10 was observed when the protein was detected using another well-characterized anti–LN-$\alpha5$ chain antibody, 4G6 (28) (unpublished data). Furthermore,

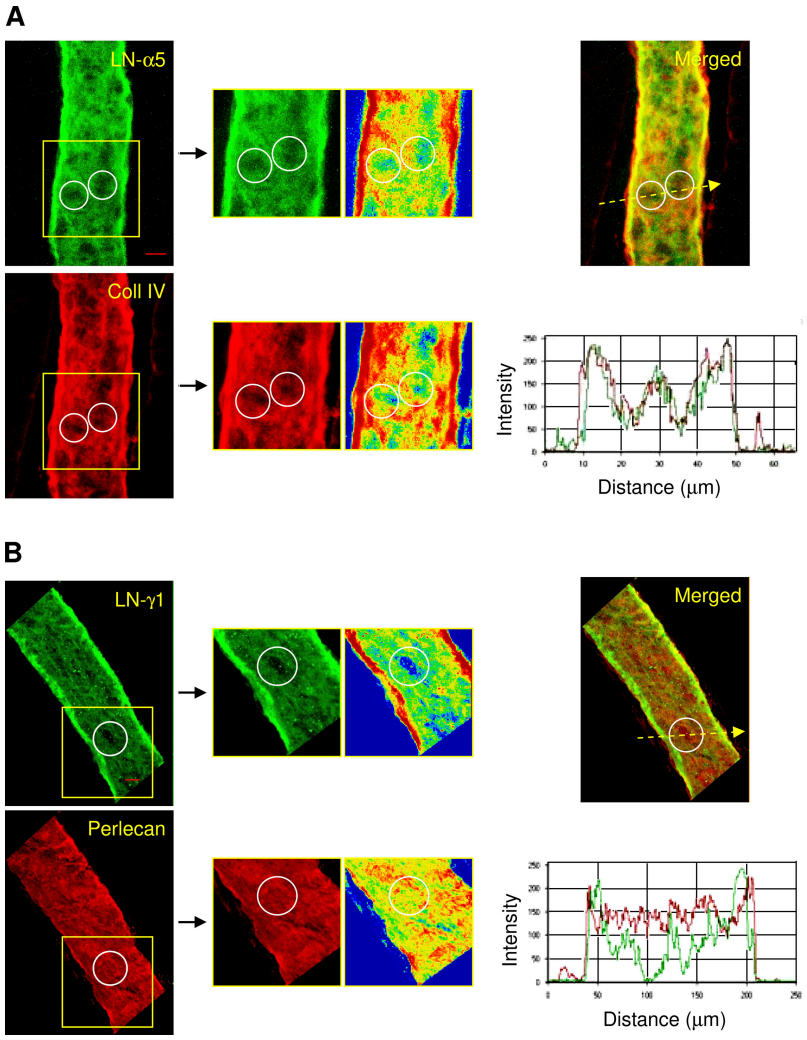

Figure 2. Laminin 10 LE regions also express low levels of collagen IV but continuous expression of perlecan. The panels show unstimulated cremasteric venules double stained as follows. (A) Laminin $\alpha5$ chain (detecting laminin 10) and collagen IV and (B) laminin $\gamma1$ chain (constituent of both laminins 8 and 10) and perlecan. In both panels, the vessel segment indicated in the boxed area is shown at a higher magnification (together with its corresponding image intensity profile) to better illustrate the expression profiles of molecules under investigation (middle). The positions of the same representative laminin LE sites are shown in all four middle images in each panel. On the right in each panel, histogram plots of a latitudinal section of the vessel, cutting through selected laminin LE sites, are shown to illustrate the colocalization of laminin LE sites with collagen IV LE regions (A, right) and the continuous expression of perlecan at laminin LE sites (B, right). In these panels, laminin fluorescence intensity (arbitrary units) is shown in green and collagen IV and perlecan intensities are shown in red. Each image is representative of three to five vessels/tissue (n = 3–4 mice per group). Bar, 10 μm.

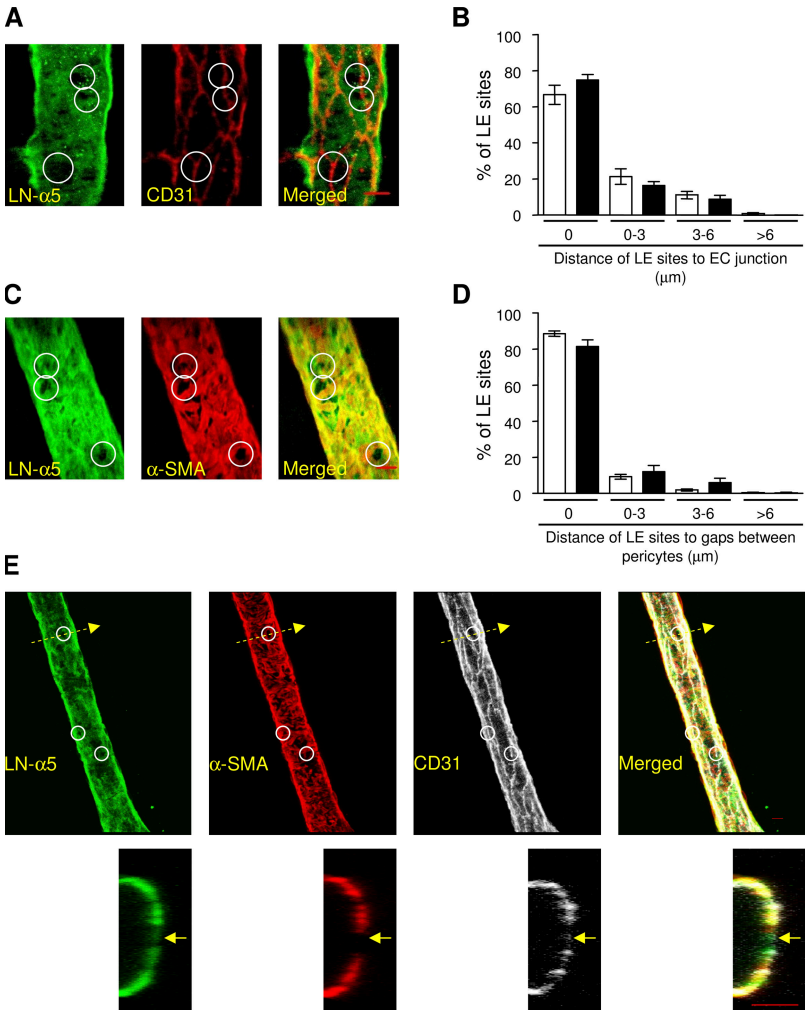

Figure 3. Localization of laminin 10 and collagen IV LE regions with endothelial cell junctions and gaps between pericytes. To investigate the localization of laminin 10 (as detected by an anti–LN-α5) and collagen IV LE regions in relation to endothelial cells and pericytes, unstimulated cremaster muscle tissues were double stained for the extracellular matrix protein of interest together with either CD31 (as an endothelial cell marker) or α-SMA (as a pericyte marker). All images shown are from semi-vessels. (A) Representative three-dimensional images of venules immunostained for LN-α5 and CD31. White rings indicate the position of selected LE regions, some indicating a high association with endothelial cell junctions. (B) Graph shows the percentage of laminin 10 (white bars) and collagen IV (black bars) LE sites at different distances from their closest endothelial cell junction. (C) Representative three-dimensional images of venules immunostained for LN-α5 and α-SMA. White rings indicate the position of selected LE regions clearly indicating the high association of their localization with gaps between pericytes. (D) The graph shows the percentage of laminin 10 (white bars) and collagen IV (black bars) LE regions at different distances from pericyte gaps. In these studies, a total of 650 LE sites, observed in three to five vessels in three to four mice per group, were analyzed. (E) A representative venule triple stained for LN-α5, α-SMA, and CD31 is shown, indicating the high association of laminin 10 LE regions (selected examples shown by rings) with pericyte gaps and endothelial cell junctions. The bottom panels were obtained by cutting a cross section of the venule (1-μm thick) along the indicated line through a selected LE region. These representative images further indicate the direct colocalization of a laminin 10 LE site with an α-SMA–negative region and in close proximity of an endothelial cell junction (as indicated by discrete regions of high fluorescence intensity). Bar, 10 μm.

antibodies directed against the laminin γ1 chain (a rat anti–mouse γ1 mAb, 3E10, and a rabbit anti–mouse γ1 polyclonal, 454) (29), which would detect both laminin 10 and laminin 8, exhibited similar staining profiles to that observed with anti–LN-α5 chain antibodies (Fig. 1 B and not depicted). A similar heterogeneous expression profile was observed when tissues were stained for collagen IV and nidogen-2 (Fig. 1 B). Interestingly, laminin 10 LE sites were directly colocalized with LE regions within the collagen IV network (Fig. 2 A), but exhibited continuous expression of perlecan (Fig. 2 B), demonstrating that LE regions express normal levels of certain extracellular matrix proteins. LE regions were also observed in venules of tissues obtained from animals treated with intravenous cocktail of protease inhibitors immediately before tissue collection, in tissues maintained in a cocktail of protease inhibitors throughout the

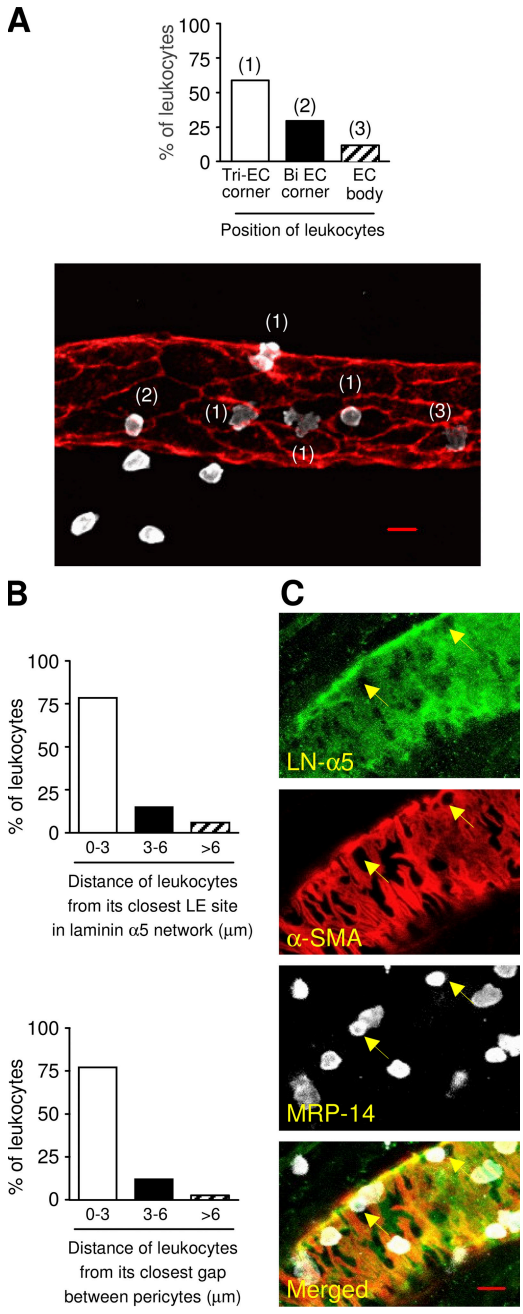

Figure 4. Association of neutrophils in IL-1β–stimulated tissues with endothelial cell junctions, LE sites in the laminin 10 network, and gaps between pericytes. (A) IL-1β–stimulated mouse cremasteric tissues (50 ng/mouse injected intrascrotally, 4-h time point) were immunostained for the endothelial cell (EC) marker CD31 (red) and neutrophil marker MRP-14 (white). Three-dimensional images of semi-vessels of interest were captured and association of neutrophils with different EC junctions (i.e., found at tricellular or bicellular junctions) or the EC body was quantified. The graph shows the percentage of neutrophils at different positions relative to EC junctions. A representative fluorescence micrograph is shown in which examples of positions of neutrophils at tri-EC junctions, bi-EC junctions, and EC body are indicated by "(1)," "(2)," and "(3)," respectively. The corresponding bars on the graph are labeled with the same numbering scheme. For these studies, a total of 108 the percentage of neutrophils within different distance ranges from their closest LN-α5 LE sites (top) and gaps between pericytes (bottom). (C) Images show representative fluorescent micrographs of venules (semi-vessels) in IL-1β–stimulated tissues triple stained for laminin 10 (LN-α5 chain), α-SMA, and MRP-14. Selected regions of laminin LE sites are shown by arrows. Results are from four to five vessel segments/tissue ($n = 6$ cremaster muscles). Bar, 10 μm.

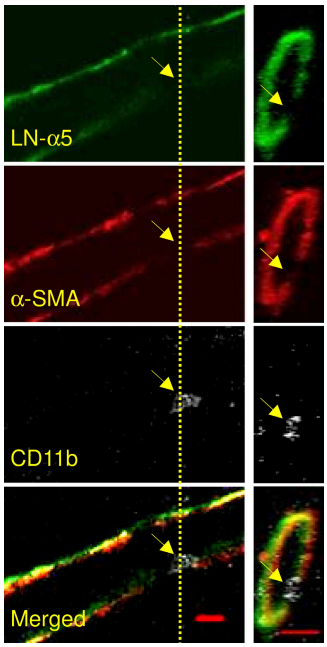

Figure 5. In IL-1β–stimulated tissues, neutrophils migrate through laminin 10 LE sites and gaps between pericytes. IL-1β–stimulated mouse cremasteric tissues (50 ng/mouse injected intrascrotally, 4-h reaction) were immunostained for laminin 10 (LN-α5 chain), α-SMA (pericyte marker), and CD11b (leukocyte marker) and analyzed by confocal microscopy. The images on the left are from a midline optical section of a three-dimensional image of a whole venule along its longitudinal axis. The images on the right were obtained by cutting a cross section of the venule along the indicated yellow line. These representative images clearly indicate colocalization of a laminin 10 LE site, a pericyte gap, and a transmigrating leukocyte (all indicated by yellow arrows). Bar, 10 μm.

fixation and staining protocol and also in frozen tissue sections as opposed to paraformaldehyde (PF)-fixed samples (unpublished data), collectively indicating that the observed tissue staining profiles were not the result of nonspecific release of leukocyte proteases during the fixation procedure.

Because laminin 10 and collagen IV are major components of venular BMs, these molecules were chosen for further characterization of their LE regions and role in neutrophil transmigration.

Characterization of LE regions

Detailed analysis of 127 random sites, as identified by the observer, in seven different tissue samples, revealed that >95% of LE sites expressed a fluorescence intensity (pixels/unit area)

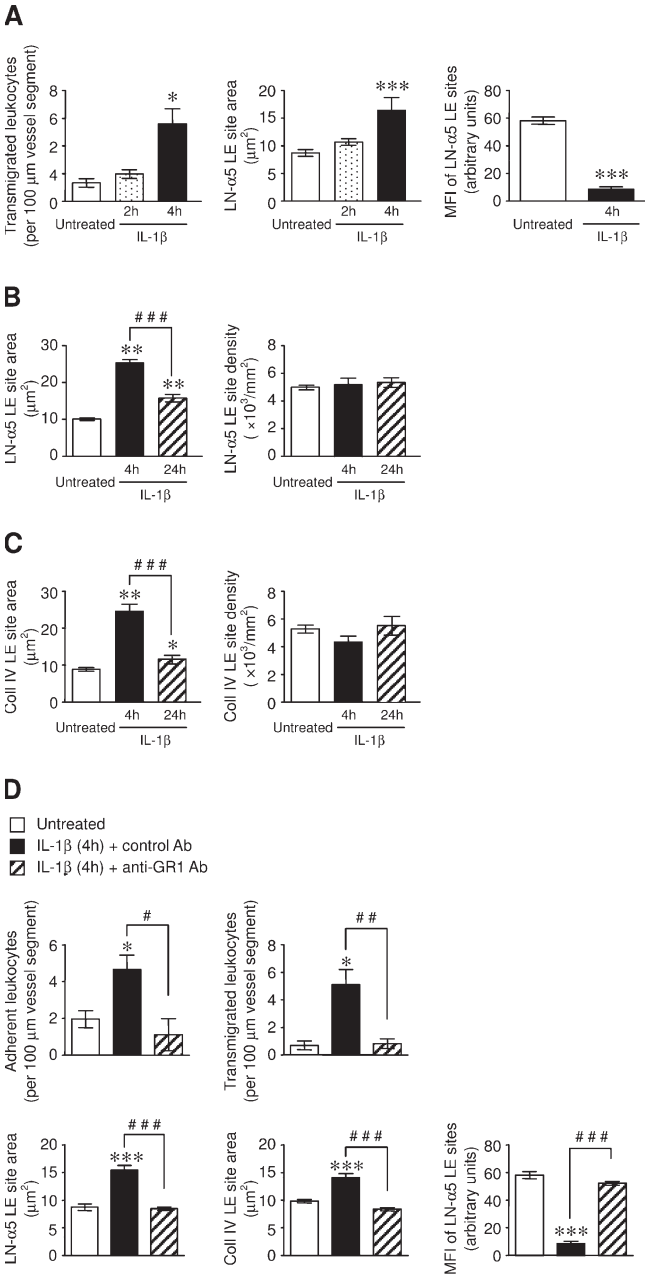

Figure 6. Average size and intensity, but not number/unit area, of LE sites in both laminin 10 and collagen IV networks is increased in IL-1β–stimulated tissues in a neutrophil-dependent manner. Leukocyte responses of firm adhesion and/or transmigration were quantified in untreated or IL-1β (50 ng/mouse)–stimulated mouse cremaster muscles by intravital microscopy at indicated time points after i.s. injection of IL-1β. In some experiments, after in vivo analysis of responses, tissues were dissected from the mice and immunostained for laminin 10 (LN-α5 chain) or collagen IV. Three-dimensional images of venules were scanned and density (number/unit area), area, and average fluorescence intensity of matrix protein LE sites were measured as described in Materials and methods. (A) The two graphs on the left show time course of neutrophil transmigration and area of LE sites within the LN-α5 network in untreated tissues and in tissues stimulated for the indicated periods with IL-1β. The graph on the right shows mean of fluorescence intensity (MFI, arbitrary units) of LE regions. (B) The graphs show the area (left) and density (right) of LE sites within the LN-α5 network in untreated tissues and in tissues stimulated for the indicated periods with IL-1β. (C) Similarly, the graphs show the area (left) and density (right) of collagen IV LE sites in untreated and IL-1β–stimulated tissues. (D) Mice were depleted of their circulating neutrophils by injection of anti-GR1 mAb and control mice were injected with an isotype-matched control mAb (100 mg i.p. for both mAbs). 24 h later, mice were injected i.s. with IL-1β (50 ng/mouse) and 4 h later leukocyte adhesion and transmigration was quantified by intravital microscopy. At the end of the in vivo test period, cremaster muscle tissues were dissected away, fixed, and immunostained for laminin 10 (LN-α5) or collagen IV and the size and/or intensity (MFI) of LE regions were quantified as detailed in Materials and methods. In all panels, a total of 316–716 LE sites from three to seven vessel segments/tissue (n = 3–4 mice per group) were analyzed. Significant differences in responses in IL-1β–stimulated tissues as compared with unstimulated tissues are indicated by asterisks, *, $P < 0.05$ and ***, $P < 0.001$. Further comparisons are shown by lines. #, $P < 0.05$; ##, $P < 0.01$; and ###, $P < 0.001$.

of <60% of the average fluorescence intensity of the vessel segment under investigation. Based on this finding, in all subsequent studies, laminin 10 LE sites were identified as regions where the average fluorescence intensity/unit area was <60% of that in the whole vessel segment, thus providing a means of normalizing identification of LE regions in different tissue samples.

The localization of the laminin 10 LE sites in relation to cellular components of venular walls, endothelial cells, and pericytes was investigated in tissue samples double stained for laminin 10 (LN-α5 chain) and CD31 (marker for endothelial cells) or α-SMA (marker for pericytes). In preliminary studies, staining of tissues with anti-CD31 and anti–α-SMA antibodies revealed the characteristic cobblestone-like staining of the cellular contours of endothelial cells (Fig. 3 A) and the patchy staining typical of pericytes (Fig. 3 C), respectively. Analysis of samples stained for laminin 10 and CD31/α-SMA by confocal microscopy indicated that within the x-y plane of 1-µm-thick optical sections, laminin 10 LE sites were closely associated with endothelial cell junctions and with gaps between pericytes. Specifically, ~70% and ~90% of laminin 10 LE sites were superimposed on endothelial cell junctions (Fig. 3, A and B) and α-SMA–negative regions (marking gaps between pericytes) (Fig. 3, C and D), respectively. Further evidence for localization of laminin 10 LE sites with endothelial cell junctions and pericyte gaps was obtained from tissues triple stained for LN-α5 chain, CD31, and α-SMA (Fig. 3 E). Fig. 3 E (bottom) also shows the expressions of these molecules within a laminin 10 LE region, as observed within a cross section of the venule, clearly indicating localization of the LE site with an α-SMA–negative region. Additional characterization of venular laminin 10 LE regions indicated that they were of variable shape but had an average area of 9.29 ± 0.53 µm² and were expressed at a density of 5,020 ± 140/mm² (199 sites in 14 venules in 3 tissues); this equates to an average of ~30 LE sites within a 100-µm vessel segment of a 20-µm-diameter venule. Collagen IV LE sites were of comparable localization, size and density (Fig. 3, B and D, and Figs. 6 and 7).

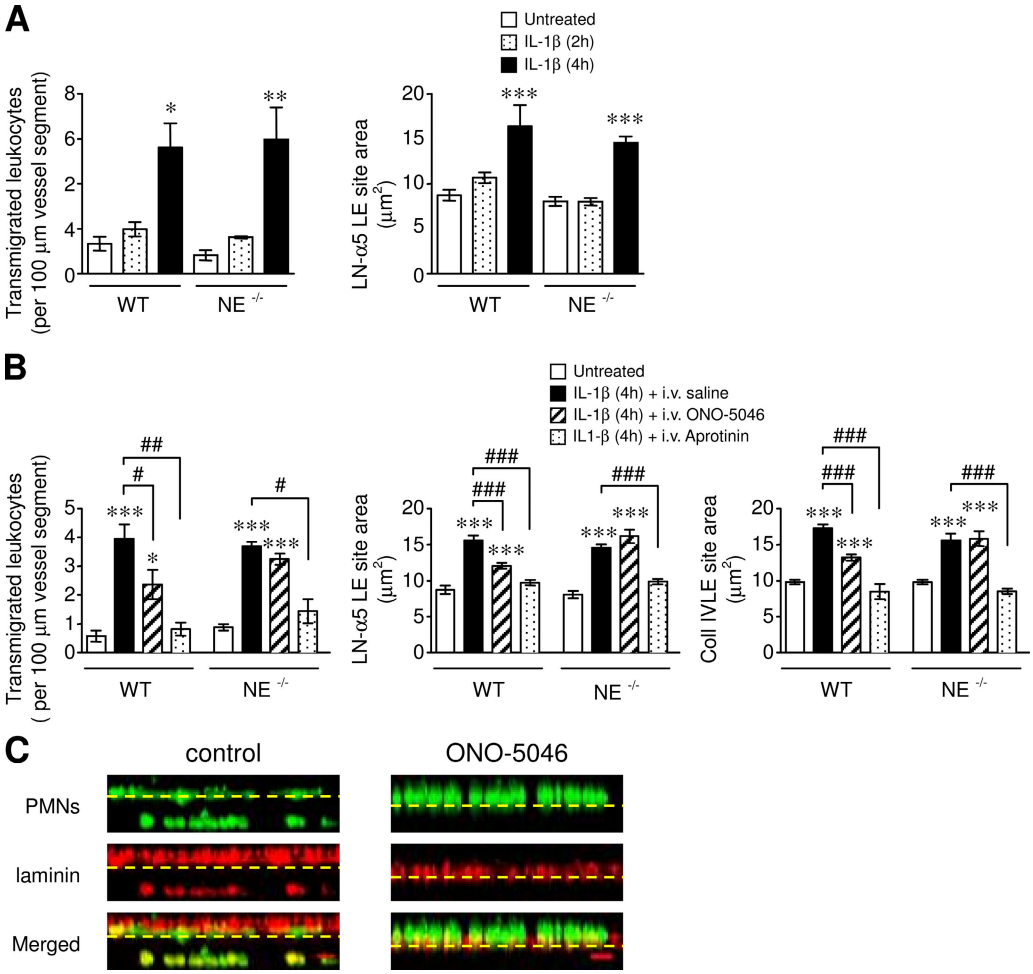

Figure 7. Role of NE in laminin disruption in vivo and in vitro. (A) WT or $NE^{-/-}$ mice were injected via the intrascrotal (i.s.) route with IL-1β (50 ng/mouse) (control mice were untreated). (B) WT or $NE^{-/-}$ mice were injected with i.s. IL-1β (control mice were untreated) and 2 h later a continuous infusion of the specific NE inhibitor, ONO-5046, or aprotinin (see Materials and methods for dosing regimes) was injected to the mice (control mice received an infusion of saline). In all experiments, 2–4 h after injection of IL-1β (as indicated), leukocyte transmigration in cremasteric venules was quantified by intravital microscopy as detailed in Materials and methods. At the end of the in vivo test period, cremaster muscles were dissected away from mice, fixed, and immunostained with an anti–LN-α5 Ab and/or anti–collagen IV (coll IV) Ab and the size of LE regions was evaluated as detailed in Materials and methods. In all panels, a total of 300–716 LE sites, from 3 to 22 vessel segments, using three to nine mice per group were analyzed. Significant differences in responses in IL-1β–stimulated tissues as compared with unstimulated tissues are indicated by asterisks (*, $P < 0.05$; **, $P < 0.01$; and ***, $P < 0.001$) and further comparisons are shown by cross-hatched lines (#, $P < 0.05$; ##, $P < 0.01$; and ###, $P < 0.001$). (C) 96-well NeuroProbe chemotaxis chambers were used for investigating neutrophil migration through laminin-1–coated filters as detailed in Materials and methods. In brief, bone marrow–derived mouse neutrophils (untreated or treated with 50 μM of the NE inhibitor ONO-5046) were placed on top of the filters with IL-8 (10^{-7} M) in the bottom wells. After an incubation period of 1.5 h at 37°C, the filters were immunostained for laminin-1 (red) and the leukocytes were stained with the nuclear dye SytoxGreen (green). Results are representative of three independent experiments. Bar, 10 μm.

Neutrophils preferentially migrate through LE regions

To address the potential association of laminin 10 LE sites with neutrophil transmigration through the BM, cremaster muscles injected with IL-1β were investigated. Immunofluorescent staining of IL-1β–stimulated tissues with antibodies against MRP-14 (a cytoplasmic Ca^{2+} binding protein expressed at high concentrations within neutrophils [30] used as a neutrophil marker) and CD31 indicated a significant increase in neutrophil attachment to venular endothelial cells in IL-1β–injected (as compared with saline injected) tissues. Of these, 59% were detected at endothelial cell tricellular corners and 29% were detected at bicellular corners, in agreement with previous reports (31) (Fig. 4 A). To further localize the position of transmigrating neutrophils in relation to laminin 10 LE sites and pericytes, tissues were triple stained for CD11b or MRP-14 (leukocyte markers), LN-α5, and α-SMA. In these tissues, confocal analysis of optical sections indicated that >75% of all leukocytes associated with the vessel wall were within 0–3 μm of a laminin 10 LE site and a gap between pericytes (Fig. 4, B and C). In addition,

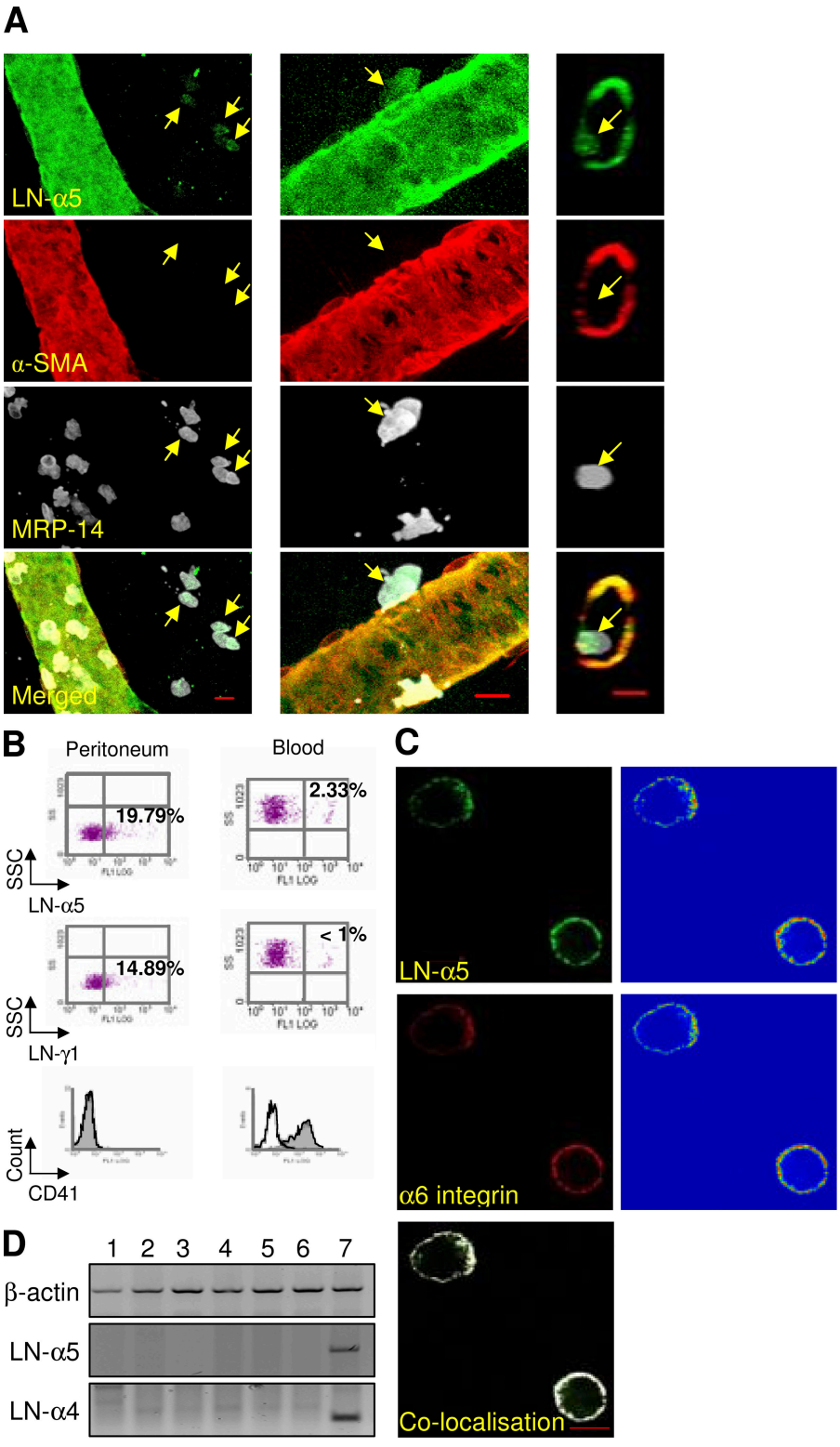

Figure 8. Transmigrated neutrophils carry laminin on their cell surface. (A) IL-1β–stimulated mouse cremasteric muscles were immunostained for LN-α5 chain, α-SMA (pericyte marker), and MRP-14 (neutrophil marker), and three-dimensional images of whole vessels were collected by confocal microscopy. The fluorescence micrographs show cross-sectional images and three-dimensional images of the same venular segment in which a transmigrating neutrophil (arrows) is shown to be LN-α5 chain positive. Bar, 10 μm. (B) Mice were injected i.p. with thioglycollate and peritoneal cells were harvested at 2 h after administration of the stimulus. Cell surface expression of LN-α5 and -γ1 subunits on blood or peritoneal neutrophils were quantified by flow cytometry and results are shown as scatter profiles. The numbers in each scatter profile

with this approach, clear evidence was obtained for migration of neutrophils through laminin 10 LE sites and gaps between pericytes (Fig. 5).

Transmigration results in remodeling of the LE regions

We next investigated whether emigrating neutrophils altered the size, protein content, or density (number/unit area) of LE regions. In IL-1β–stimulated cremaster tissues, kinetics of neutrophil transmigration was directly associated with a time-dependent increase in size of LE regions, as compared with unstimulated tissues (Fig. 6 A). Specifically, 4 h after injection of IL-1β, a time point at which significant neutrophil transmigration was noted, a significant increase of 88% in the average size of laminin 10 LE regions was detected, as compared with the average size of LE sites in unstimulated cremasters (Fig. 6 A). Interestingly, in the same regions, the enlarged laminin 10 LE sites had a significantly lower fluorescence intensity (Fig. 6 A), indicating a reduced level of immunoreactive laminin 10. The observed increase in size of laminin 10 LE regions was a transient response and returned toward basal levels by 24 h after injection of IL-1β (Fig. 6 B). Despite the aforementioned data, no difference in the number/unit area of laminin 10 LE regions was noted at any time point investigated up to 24 h after injection of IL-1β (Fig. 6 B). Similar transient changes in the size and/or intensity of LE sites, but not their density, were observed when the tissues were stained for collagen type IV (Fig. 6 C and not depicted) or when stimulated with TNFα as opposed to IL-1β (not depicted).

To investigate the role of neutrophils in the remodeling of LE regions, the effect of neutrophil depletion was investigated. Pretreatment of mice with the antineutrophil mAb anti-GR1 24 h before intrascrotal injection of IL-1β led to >87% depletion of circulating neutrophils. In these mice (but not in control mAb-treated animals), there was no detectable leukocyte adhesion or transmigration 4 h after administration of IL-1β as observed by intravital microscopy (Fig. 6 D). Furthermore, analysis of venules of these mice indicated no increase in the size of laminin 10 or collagen IV LE regions or change in their protein levels (Fig. 6 D), providing direct evidence for the involvement of neutrophils in the aforementioned BM remodeling events.

Role of a proteolytic event?

A potential mechanism by which neutrophils may increase the size of extracellular matrix protein LE sites is via proteolytic cleavage and subsequent transportation of extracellular matrix fragments on the surface of transmigrating neutrophils. Because we have previously found that transmigrated neutrophils express NE on their cell surface (32), the size of laminin 10 LE regions in IL-1β–stimulated cremaster muscles in NE-deficient mice and WT mice treated with a specific NE inhibitor, ONO-5046 (Sivelestat) (33), was investigated. In agreement with our previous findings (32, 34), in NE-deficient mice, IL-1β–stimulated leukocyte transmigration was not significantly different (in magnitude or kinetics) from that seen in WT animals (Fig. 7 A). Furthermore, a similar increase in the size of laminin 10 LE regions was detected in both WT and NE-deficient mice after injection of IL-1β, though NE-deficient mice appeared to exhibit a small but nonsignificant delay in exhibiting this response. In contrast, in WT animals treated intravenously with ONO-5046, IL-1β–induced leukocyte transmigration was significantly inhibited (46.9% reduction; $P < 0.05$) and a significant reduction in the average size of both laminin 10 (51.3% reduction; $P < 0.001$) and collagen IV (54.9% reduction; $P < 0.001$) LE regions was noted as compared with control mice (Fig. 7 B). Interestingly, ONO-5046 had no inhibitory effects in NE-deficient mice, indicating selectivity of this compound for NE. Furthermore, the broad spectrum serine protease inhibitor, aprotinin, when administered intravenously, significantly suppressed IL-1β–induced leukocyte transmigration and increased in size laminin and collagen IV LE regions in both WT and NE-deficient mice (Fig. 7 B), suggesting the existence of developmental compensation in the NE-deficient animals.

Using an in vitro transmigration assay, additional evidence was obtained for the ability of neutrophils to cleave laminin in an NE-dependent manner (Fig. 7 C). In this assay, IL-8–induced transmigration of mouse neutrophils through laminin-1 (composed of α1β1γ1 chains)–coated filters was investigated as described previously (32). Analysis of the filters after transmigration by confocal microscopy showed that transmigrated neutrophils were positive for laminin (Fig. 7 C), indicating that cells migrating through laminin-coated filters can carry fragments of the protein on their cell surface. Furthermore, in line with the aforementioned findings, neutrophil transmigration in this assay was inhibited by the NE inhibitor ONO-5046.

In vivo evidence was also obtained showing that transmigrated neutrophils express laminin 10 on their cell surface both in the cremaster muscle (Fig. 8 A) and peritonitis models (Fig. 8 B). In the former, analysis of 425 transmigrated neutrophils in 22 random fields of view in four immunostained tissue samples indicated that ∼20% of the cells were

shown in bold represent percent of positive cells. The cell samples were also stained for CD41 (platelet marker) at 4 h after stimulation. The results are representative of three independent experiments. (C) IL-1β–elicited transmigrated peritoneal leukocytes were immunostained for LN-α5 chain and α6 integrin and analyzed by confocal microscopy. Representative images of midlevel sections of cells are shown together with their corresponding intensity profiles (right). Colocalization of LN-α5 and α6 integrin was better indicated using the LSM 5 Pascal software that allows colocalized pixels of the two fluorescence channels to be visually shown by a white mask superimposed onto the original RGB image. (D) RT-PCR analysis for β-actin, LN-α5, and α4 chains from purified neutrophils (lanes 1, 3, 5) and residual mononuclear cells (lanes 2, 4, 6) harvested from thioglycollate (lanes 1–4) or IL-1β (lanes 5–6) elicited peritonitis studies. Confluent murine cardiac endothelial cells (lane 7) were used as a positive control.

LN-α5 positive. In the peritonitis model, using indirect immunofluorescent staining and FACS analysis, no significant laminin α5 or γ1 chain positive neutrophils were detected in blood samples; however, a significant increase in positive neutrophils was detected in the peritoneal exudates of IL-1β– or thioglycollate-treated mice (Fig. 8, B and C, and not depicted). In the thioglycollate model, this response appeared to be maximal at 1–2 h after injection of the inflammatory stimulus (~15–20% positive cells) and declined to ~9% positive cells by 4 h (unpublished data). Similar results were obtained when samples were stained with an anti–LN-α4 chain antibody (unpublished data), detecting laminin 8. Interestingly, analysis of transmigrated peritoneal neutrophils by confocal microscopy indicated that the cell surface staining for laminin (detected using anti–LN-α5 chain) colocalized with α_6 integrin distribution (Fig. 8 C), supporting the concept that neutrophils bind to laminins in the BM via $\alpha_6\beta_1$.

Although our results suggest that the cell surface laminin detected on transmigrated neutrophils is derived from the vascular BM, several other possibilities exist. Because human platelets and neutrophils have been reported to express laminin 8 (35, 36), we considered the possibility that the laminin expression detected in our models was either associated with platelets adherent to the neutrophil population or was mobilized from neutrophil intracellular stores after transmigration. To address the former, platelet contamination of blood and peritoneal cells was analyzed by FACS using GPIIb (CD41) as a platelet marker. In contrast with the neutrophil population in blood samples that were positive for CD41, peritoneal neutrophils were CD41 negative (Fig. 8 B), indicating that the laminin on the surface of transmigrated neutrophils was not the result of platelet contamination. To address the latter possibility, we performed intracellular immunostaining for laminin 8 (LN-α4 chain) and laminin 10 (LN-α5 chain), followed by FACS analysis of blood and peritoneal neutrophils and found no evidence of preformed intracellular sources of laminins in mouse neutrophils (unpublished data). In addition, using a pan-antilaminin polyclonal antibody, no evidence of laminin protein was found in mouse bone marrow or blood-derived neutrophils, as analyzed by Western blot analysis, whereas laminin presence was confirmed in lysates of human neutrophils (unpublished data) (36). Finally, RT-PCR failed to detect the presence of mRNA for laminin 8 or laminin 10 (using LN-α4 and LN-α5 chain–specific primers, respectively) in mouse peritoneal neutrophils while showing clear presence of message for these proteins in mouse endothelial cells (Fig. 8 D).

DISCUSSION

Since the invention of electron microscopy, it has been known that the perivascular BM acts as a distinct but transient barrier to emigrating leukocytes (16, 18). However, the same studies also noted the absence of visible damage to the perivascular BM at sites of leukocyte migration, raising many questions related to the potential mechanisms involved. Since then, because of the difficulties in modeling the venular BM in vitro and the complexities of studying leukocyte transmigration in vivo, very little advancement has been made in understanding the mechanism by which leukocytes migrate through the perivascular BM at sites of inflammation. The findings of the present study provide evidence for the existence of regions within the venular BM, where the expression of certain BM constituents is lower than the average expression in the venular wall. These regions, which we have termed LE sites, were found to be directly associated with gaps between pericytes and appeared to be preferentially used by migrating neutrophils. Furthermore, the study provides evidence to indicate that transmigrating neutrophils can induce BM remodeling by inducing a transient enlargement of LE sites, a response that may facilitate the migration of neutrophils through the LE regions. Collectively, the present findings suggest a mechanism by which neutrophils can penetrate the perivascular BM without gross and irreversible disruption of the venular wall structure.

To address the mechanism by which neutrophils penetrate the vascular BM, the distribution of key BM constituents in venules of both unstimulated and cytokine-stimulated tissues were investigated with the aim of detecting potential differences specifically at sites of neutrophil transmigration. For this purpose, expressions of laminin 10, collagen IV, nidogen-2, and perlecan were investigated in venules of the mouse cremaster muscle. By choosing to investigate the expression of these molecules in whole mount tissues by immunofluorescent confocal microscopy, we were able to address localization of major vascular BM components in relation to the cellular components of the vessel wall in three dimensions. The results consistently indicated a heterogeneous expression profile of laminin 10, collagen IV, and nidogen-2 in the walls of 20–40-μm diameter postcapillary venules but not arterioles, an expression profile that was the result of the existence of clear LE regions. Of importance, laminin 10 and collagen IV LE regions were colocalized although continuous staining for perlecan was noted in these regions, indicating that LE sites do not lack BM but are regions in which there is less expression of selective BM constituents.

Image analysis of tissues stained for laminin 10 and collagen IV indicated that LE regions within the networks of these extracellular matrix proteins exhibit comparable profiles in terms of density (number/unit area) and size. Furthermore, localization of LE regions with respect to the endothelial and pericyte compartments of the vascular wall revealed a close association with endothelial cell junctions and an even stronger association with gaps between pericytes, with almost 100% of the LE regions being within 0–3 μm of pericyte gaps. These results are consistent with the idea that both endothelial cells and pericytes may contribute to the vascular basement membrane, as suggested from in vitro experiments (5, 6).

Analysis of IL-1β–stimulated cremaster muscles revealed a close association between LE sites and sites of neutrophil transmigration. In agreement with the findings of Burns et al. (31), the majority of leukocytes attached to venular walls were found at endothelial cell tricellular junctions (~60%),

regions reported to have discontinuous expression of tight and adherens junctions (31). Furthermore, ~75% of transmigrating and/or transmigrated neutrophils were within 0–3 μm of laminin 10 LE regions and gaps between pericytes. These results suggest that neutrophils traverse the vessel wall by preferentially migrating through sequential vulnerable regions, i.e., endothelial cell tricellular junctions, gaps between pericytes, and extracellular matrix protein LE regions within the BM. This conclusion is in line with the frequently noted observation by intravital microscopy that leukocyte transmigration appears to preferentially occur at specific points along the vessel wall, with leukocytes very often budding off from a small number of points along a vessel segment (4).

Despite the lack of detectable morphological changes by electron microscopy (16, 18), there are reports that transmigrated BM can exhibit reduced barrier function as defined by retention of macromolecules (3). To investigate whether transmigration elicited changes in the BM in our model, the average size, fluorescence intensity, and number/unit area of laminin and/or collagen IV LE regions were quantified in tissues after stimulation with IL-1β. The time course of neutrophil transmigration was directly associated with remodeling of the LE sites in that at the 4-h time point, when significant neutrophil transmigration was quantified, a significant increase in the size of LE regions was observed. Interestingly, these regions exhibited a reduced level of immunoreactive matrix protein as compared with LE sites in unstimulated tissues. No change in the number of LE regions was, however, noted in IL-1β–stimulated tissues as compared with untreated cremaster muscles. These results demonstrate that neutrophil migration through the perivascular BM does not lead to an increase in the number of LE sites, but occurs through preexisting "permissive" regions. The data presented also demonstrate that the alterations in the size of LE regions in the vascular BM are directly caused by emigrating neutrophils and are transient in nature, returning toward basal dimensions within 24 h after initiation of transmigration. The latter reinforces the fact that the vascular BM is a dynamic and not a static and rigid structure (6, 28). Vascular endothelial cells have been reported to respond rapidly to proinflammatory cytokines with altered expressions of the vascular laminin isoforms, laminins 8 and 10, resulting in local changes in the underlying basement membrane (6, 13, 37) and adaptation to the physiological needs of the tissue. The findings presented here are in accordance with the observations of Huber and Weiss (3) who using an in vitro model of the vessel wall reported BM defects induced by transmigrating neutrophils, as defined by a loss of permeability function. This induced defect appeared to be transient and was inhibited by both protein and mRNA synthesis inhibitors.

Although it is considered controversial (3, 38), proteolytic cleavage of BM constituents is a commonly proposed mode of leukocyte penetration of BM barriers. Because the serine protease neutrophil elastase is known to be expressed on the cell surface of transmigrating neutrophils both in vitro (39) and in vivo (32) and has been implicated in neutrophil migration through the BM (17, 32, 39, 40), the role of this protease in disruption of the BM in IL-1β–stimulated tissues was investigated. Data presented here implicate neutrophil-derived serine proteases such as NE in increased size of laminin 10 LE regions during cytokine-induced neutrophil transmigration. Together with our previous findings (32), these results suggest that NE may facilitate neutrophil migration through the BM by selective cleavage events without overt disruption of its structure. However, because remodeling of the BM was shown to be directly dependent on neutrophil transmigration (Fig. 6 D), it is also possible that protease blockers inhibited enlargement of the LE regions as a result of inhibiting neutrophil transmigration (e.g. through suppressing physical rather than catalytic alterations in the BM). The mechanisms by which NE may mediate neutrophil transmigration and/or BM remodeling, directly or indirectly, is at present unclear, especially in the light of the broad substrate specificity of NE (41). It is of course highly probable that NE may have indirect roles in mediating neutrophil transmigration, for example, via activation of other leukocyte proteases such as MMP-9 (17) or generation of chemotactic fragments by selective cleavage of BM constituents (42–44) or cellular receptors. However, NE may also play a direct role in mediating neutrophil transmigration, possibly via cleavage of BM constituents (17, 40). In this context, although at present it is unclear whether NE can directly cleave the vascular laminins, laminin 8 and 10, evidence for this possibility was suggested in experiments showing that neutrophils transmigrating through laminin-1–coated filters carried laminin on their cell surface in an NE-dependent manner. Furthermore, in vivo, transmigrated neutrophils were laminin positive. Specifically, in both the cremaster muscle model and in peritonitis models, a small percentage of emigrated neutrophils (~15–20%) were found to express laminin on their cell surface. It is conceptually possible that the small number of laminin-expressing cells represent the leading-front neutrophils that may act as "path clearers" for the "late arrivals," the latter being able to traverse the BM without the need for further cleavage/carriage of matrix proteins (i.e., remain laminin negative). Interestingly, in peritoneal neutrophils, the cell surface laminin was colocalized with α_6 integrins supporting the concept that $\alpha_6\beta_1$ plays an important role in the adhesive interaction of neutrophils with vascular laminins (23, 37). Of importance, although it has previously been reported that human neutrophils contain intracellular stores of laminin 8 (36), we found no evidence for intracellular laminin protein or mRNA in mouse neutrophils. These results suggest that cell surface laminins on transmigrated neutrophils were not derived from the neutrophils themselves and that very likely their source was the vascular BM.

In summary, because the perivascular BM acts as a formidable but transient barrier to emigrating leukocytes, mechanisms must exist by which leukocytes can penetrate this structure without causing an irreversible damage to its intricate network and compromising its barrier function. The present study reports for the first time on regions within the

BM of murine cremasteric venules where the deposition of selective BM components is low. These regions are in close association with gaps between pericytes and appear to be preferentially used by neutrophils migrating through the perivascular BM, a response that may be facilitated by interaction of neutrophil cell surface leukocyte integrins (e.g., $\alpha_6\beta_1$) and NE with BM components. Although, at present, it is unclear whether other leukocyte subtypes use a similar mechanism for penetration of venules, as there is evidence to indicate that distribution of vascular laminins can define sites of T cell transmigration in vivo (29), the expression profile of venular BM constituents may represent a previously unappreciated and general mechanism by which leukocyte emigration is regulated.

MATERIALS AND METHODS

Animals

WT C57BL/6 mice (~25 g) were purchased from Harlan-Olac. Neutrophil elastase–deficient ($NE^{-/-}$) mice were a gift from S. Shapiro (Harvard Medical School, Boston, MA).

Induction of inflammation and intravital microscopy of cremasteric venules

Male mice were injected via the intrascrotal (i.s.) route with saline or recombinant murine IL-1β (50 ng/mouse; R&D Systems). In studies involving aprotinin (Sigma-Aldrich) or the NE inhibitor ONO-5046 (ONO Pharmaceuticals), 2 h after injection of the cytokine, mice were anaesthetized as described previously (45) and a bolus of saline (control, followed by continuous infusion of saline at 200 μl/h using a syringe pump; Harvard Instruments), aprotinin (100 KIU/kg, followed by continuous infusion of 100 KIU/kg/h), or ONO-5046 (50 mg/kg, followed by 50 mg/kg/h) were administered via the jugular vein for a further 2 h. Neutrophil depletion was induced by injecting 100 mg i.p. of the anti-GR1 antibody RB6-8C5 (BD Biosciences) 24 h before i.s. administration of IL-1β. Control animals received an isotype-matched control antibody (R&D Systems). To determine blood neutrophil counts, as described previously (46), tail vein blood samples were collected from mice before and 24 h after the injection of the antibodies. Cremaster muscles were surgically exteriorized and in all studies events within the microvascular bed were quantified 2–4 h after i.s. injection of IL-1β as observed using an upright fixed-stage microscope (Zeiss Axioskop FS; Carl Zeiss MicroImaging). Leukocyte responses of rolling, firm adhesion, and extravasation in postcapillary venules of 20–40 μm diameter were quantified as described previously (45). Leukocyte transmigration was defined as the number of leukocytes in the extravascular tissue across a 100-μm vessel segment and within 50 μm of the vessel of interest. Of relevance, we have previously found that >90% of transmigrated leukocytes in IL-1β–stimulated cremaster muscles (4-h reaction), as analyzed by electron microscopy, are neutrophils (45). All animal studies were approved by Imperial College London's local ethical committee and were performed according to the directives of the UK Home Office Animals (Scientific Procedures) Act, UK (1986).

Immunostaining of mouse cremaster muscles

Cremaster muscles from mice used in the aforementioned experiments, from untreated mice, or from mice 2, 4, or 24 h after intrascrotal injection of IL-1β were dissected away from animals, fixed in PF, and immunostained as described previously (32). In brief, after being blocked and permeabilized in PBS supplemented with 20% horse serum and 0.5% Triton X-100 for 1 h at room temperature, tissues were incubated with primary antibodies (see the list below) at room temperature overnight, followed by incubation with appropriate secondary antibodies conjugated to Alexa Fluor 488, 568, or 633 (Invitrogen) at room temperature for 3 h. In experiments where tissues were triple stained, a third immunostaining step was added at room temperature for 3 h using directly conjugated primary antibodies. The following primary antibodies were used: rat anti–mouse laminin α5 chain (4G6) (28), rabbit anti–mouse laminin α5 chain (405) (46), rat anti–mouse γ1 chain (3E10) (37), rabbit anti–mouse laminin γ1 chain Ab (454) (37), rabbit anti–mouse perlecan (289) (26), and rabbit anti–mouse nidogen-2 (534) (27). Rabbit anti–mouse collagen IV polyclonal Ab (Abcam) was obtained commercially. To label leukocytes and endothelial cells, a rat anti–mouse MRP-14 (2B10; a gift from N. Hogg, Cancer Research UK, London, UK) and a rat anti–mouse CD31/CD31 (MEC13.3; BD Biosciences) were used, respectively. The following directly conjugated antibodies were used in experiments involving triple staining of tissues: Alexa Fluor 647–labeled rat anti–mouse CD11b Ab (clone M1/70, BD Biosciences) and Cy3-labeled mouse α-SMA mAb (clone 1A4, 1:200 diluted; Sigma-Aldrich) to detect leukocytes and pericytes, respectively. In all studies, appropriate control Abs were used in parallel with the specific primary antibodies. Samples were viewed using a Zeiss LSM 5 PASCAL confocal laser-scanning microscope as detailed in the next paragraph.

Analysis of tissues by confocal microscopy

Immunostained tissues were mounted on glass slides and observed at RT using an LSM 5 PASCAL confocal laser-scanning microscope (Carl Zeiss MicroImaging, Inc.). Typically, multiple optical sections of tissue samples, running through the whole depth of the tissue, were captured with the software's automatic scanning mode using as far as possible the same settings for all samples investigated. Z-stack digital images were collected optically at every 1-μm depth using multiple track scanning mode, saved, and used for three-dimensional reconstruction analysis using the LSM 5 Pascal software (version 3.2). Several analyses were performed as described in the following two paragraphs.

Localization and expression profile of extracellular matrix molecules. Three-dimensional images of vessels were split in the middle along the longitudinal axis and images of "semi-vessels" were analyzed for fluorescence intensity measurements. To investigate the expression profile of specific molecules within immunostained samples, intensity profiles of regions of interest were measured and compared with average intensity of the entire vessel within the same field of view for each molecule. For this purpose, regions of interest (immunoreactive and nonimmunoreactive) within three-dimensional images of semi-vessels were identified manually and their area, density, and fluorescence intensity (in terms of pixels) were measured using the LSM 5 Pascal software. In addition, the value of total fluorescence intensity of region of interest was totaled and an average fluorescence intensity/unit area for each region was further calculated using the statistics software GraphPad Prism 4. Intensity changes were presented graphically in two ways: (a) RGB images were converted to gray-scale images, in which color codes from red to blue were used to indicate intensities of pixels from high to low, respectively, and (b) histograms of fluorescence intensity (in arbitrary units) versus distance were plotted for selected latitudinal sections of venules to indicate the intensity profile of specific regions (LE sites) along a vessel. The distance of matrix protein LE sites to its closest endothelial cell junction or gaps between pericytes were also measured.

Localization of leukocytes. Three-dimensional images of semi- or whole vessels were captured from tissues immunostained with markers for neutrophils (CD11b or MRP-14), endothelial cells (CD31/CD31), pericytes (α-SMA), and/or laminin 10 (LN-α5 chain). Three-dimensional images were commonly observed at different angles so that the position of neutrophils relative to vessel walls could be studied and displayed more accurately. Distance of adherent/transmigrating neutrophils relative to endothelial cell junctions, to laminin LE regions or to gaps between pericytes was also measured and represented as the percentage of cells detected at defined distances away from these sites.

Peritonitis models

Mice were injected i.p. with 1 ml of PBS plus 4% thioglycollate (Sigma-Aldrich) or IL-1β (100 ng/cavity) and killed 1–4 h later by CO_2 asphyxiation and peritoneal cavities were lavaged using ice-cold PBS (supplemented with 0.25% BSA and 2 mM EDTA).

Immunostaining of mouse blood and peritoneal leukocytes and analysis by flow cytometry and confocal microscopy

Blood samples and purified peritoneal leukocytes were indirectly immunostained and analyzed by flow cytometry and confocal microscopy. For flow cytometry, after blocking Fc receptors (2.4G2; BD Biosciences), samples were incubated for 30 min with FITC-conjugated anti–mouse antibodies directed against GR1, F4/80, or CD41 (BD Biosciences) for the identification of neutrophils, macrophages, and platelets, respectively, or with the anti–mouse antibodies against LN-α4 (377), LN-α5 (405), or LN-γ1 (454) chains for 30 min at 4°C. Cells were washed and incubated for 30 min with appropriate secondary Abs (Invitrogen). Samples were analyzed with an EPICS XL flow cytometer (Beckman Coulter) and neutrophil populations were identified based on cellular morphology and Gr-1^+/F4/80^- phenotype.

To analyze samples by confocal microscopy, purified cells were fixed in 2% PF and incubated with a rat anti-α_6 integrin mAb (GoH3; BD Biosciences) and rabbit anti–mouse LN-α5 chain (405) Ab at room temperature for 30 min. The binding of these antibodies was detected by incubations with an Alexa Fluor 633–conjugated goat anti–rat IgG and an Alexa Fluor 488–conjugated goat anti–rabbit IgG, respectively. To identify neutrophils, the cell samples were further stained by the nuclear dye DAPI. Samples were observed using a Zeiss LSM 5 PASCAL confocal laser-scanning microscope as described in a previous paragraph. As well as imaging fluorescence intensities associated with each molecule individually, an image representing colocalization of molecules (in terms of colocalized pixels) was generated using the Zeiss LSM 5 Pascal software and shown as a white mask on the original RGB image.

RT-PCR

Total RNA was extracted using NucleoSpin RNA II kit (ABgene) from purified peritoneal PMNs (>90% purity), residual peritoneal mononuclear leukocytes, or a conditionally immortalized murine cardiac endothelial cell line (a gift from A. Randi, Imperial College London, London, England). Total RNA was reverse transcribed using SuperScript II Reverse Transcriptase (Invitrogen) and cDNAs of interest were amplified with BIOTaq DNA (Bioline) in a PTC-100 Thermocycler (Bio-Rad Laboratories), using specific primers (MWG) for LN-α5 chain (sense: 5′-ACGGCTCAGAAGGTTTCCCG-3′; antisense: 5′-CTTCAGACAGCCGCTGAACC-3′) (27) and LN-α4 chain (sense: 5′-GTCAGCTAGCGGATGCGCCTTCATGGG-3′; antisense: 5′-CAGTCGGCCGCGGCTGTGGGACAGGAGTTG-3′) (13) or β-actin (sense: 5′-GTGGGCCGCCCTAGGCACCAG-3′; antisense: 5′-CTCTTTGATGTCACGCACGATTTC-3′) as a positive control.

In vitro neutrophil transmigration assay and filter immunostaining

Bone marrow neutrophils (>80% purity) were isolated from wash-outs of femurs of mice, as described previously (34), and used in 96-well NeuroProbe chemotaxis chambers (incorporating 3-μm-pore polycarbonate filters; NeuroProbe, Inc.), as described previously (32). In brief, filters were coated with laminin-1 (15 μg/ml; Invitrogen) at 4°C overnight, and further coated with a combination of 20% murine CD31 (a gift from B.A. Imhof, University of Geneva, Geneva, Switzerland) and 80% human ICAM-1 (R&D Systems) at room temperature for 2 h. Control filters were coated with 2% BSA. Neutrophils (2×10^5 cells), untreated or treated with the NE inhibitor ONO-5046 (50 μM) were placed in the top compartments of the chemotaxis chambers. The bottom wells contained saline or IL-8 (10^{-7} M; Serotec). The chambers were incubated at 37°C in a humidified atmosphere (5% CO_2) for 1.5 h after which the filters were fixed in PF, immunostained for laminin with a rabbit anti–mouse laminin polyclonal antibody (MP Biomedicals) followed by incubation with a goat anti–rabbit secondary antibody. The filters were also stained with the nuclear dye Sytox green at 5 μM for 10 min (Invitrogen) to label the neutrophils. The filters were analyzed by confocal microscopy and imaged for three-dimensional reconstruction.

Statistics

All results are expressed as mean ± SEM. Statistical significance was assessed by one-way analysis of variance with Neuman-Keuls multiple comparison test. Where two variables were analyzed a Student's *t* test was used. $P < 0.05$ was considered significant.

This work was supported by funds from The Wellcome Trust, UK, grant no. 064920 (to S. Nourshargh); The British Heart Foundation, UK, grant no. PG/03/123/16102 (to S. Nourshargh); and the Swedish Medical Council (grant no. 621-2001-2141 (to L. Sorokin).

The authors have no conflicting financial interests.

Submitted: 16 June 2005
Accepted: 27 April 2006

REFERENCES

1. Vestweber, D., and J.E. Blanks. 1999. Mechanisms that regulate the function of the selectins and their ligands. *Physiol. Rev.* 79:181–213.
2. Alon, R., and S. Feigelson. 2002. From rolling to arrest on blood vessels: leukocyte tap dancing on endothelial integrin ligands and chemokines at sub-second contacts. *Semin. Immunol.* 14:93–104.
3. Huber, A.R., and S.J. Weiss. 1989. Disruption of the subendothelial basement membrane during neutrophil diapedesis in an in vitro construct of a blood vessel wall. *J. Clin. Invest.* 83:1122–1136.
4. Yadav, R., K.Y. Larbi, R.E. Young, and S. Nourshargh. 2003. Migration of leukocytes through the vessel wall and beyond. *Thromb. Haemost.* 90:598–606.
5. Mandarino, L.J., N. Sundarraj, J. Finlayson, and J.R. Hassell. 1993. Regulation of fibronectin and laminin synthesis by retinal capillary endothelial cells and pericytes in vitro. *Exp. Eye Res.* 57:609–621.
6. Hallmann, R., N. Horn, M. Selg, O. Wendler, F. Pausch, and L.M. Sorokin. 2005. Expression and function of laminins in the embryonic and mature vasculature. *Physiol. Rev.* 85:979–1000.
7. Dejana, E. 2004. Endothelial cell-cell junctions: happy together. *Nat. Rev. Mol. Cell Biol.* 5:261–270.
8. Muller, W.A. 2003. Leukocyte-endothelial-cell interactions in leukocyte transmigration and the inflammatory response. *Trends Immunol.* 24:327–334.
9. Imhof, B.A., and M. Aurrand-Lions. 2004. Adhesion mechanisms regulating the migration of monocytes. *Nat. Rev. Immunol.* 4:432–444.
10. Muller, W.A., S.A. Weigl, X. Deng, and D.M. Phillips. 1993. CD31 is required for transendothelial migration of leukocytes. *J. Exp. Med.* 178:449–460.
11. Feng, D., J.A. Nagy, K. Pyne, H.F. Dvorak, and A.M. Dvorak. 1998. Neutrophils emigrate from venules by a transendothelial cell pathway in response to FMLP. *J. Exp. Med.* 187:903–915.
12. Sorokin, L., W. Girg, T. Gopfert, R. Hallmann, and R. Deutzmann. 1994. Expression of novel 400-kDa laminin chains by mouse and bovine endothelial cells. *Eur. J. Biochem.* 223:603–610.
13. Frieser, M., H. Nockel, F. Pausch, C. Roder, A. Hahn, R. Deutzmann, and L.M. Sorokin. 1997. Cloning of the mouse laminin α4 cDNA. Expression in a subset of endothelium. *Eur. J. Biochem.* 246:727–735.
14. Timpl, R. 1996. Macromolecular organisation of basement membranes. *Curr. Opin. Cell Biol.* 8:618–624.
15. Hirschi, K.K., and P.A. D'Amore. 1996. Pericytes in the microvasculature. *Cardiovasc. Res.* 32:687–698.
16. Hurley, J.V. 1963. An electron microscopic study of leucocytic emigration and vascular permeability in rat skin. *Aus. J. Exp. Biol. Med. Sci.* 41:171–186.
17. Delclaux, C., C. Delacourt, M.-P. d'Ortho, V. Boyer, C. Lafuma, and A. Harf. 1996. Role of gelatinase B and elastase in human polymorphonuclear neutrophil migration across basement membrane. *Am. J. Respir. Cell Mol. Biol.* 14:288–295.
18. Marchesi, V., and H.W. Florey. 1960. Electron micrograph observations on the emigration of leukocytes. *Q. J. Exp. Physiol.* 45: 343–374.
19. Werr, J., X. Xie, P. Hedqvist, E. Ruoslahti, and L. Lindbom. 1998. β_1 integrins are critically involved in neutrophil locomotion in extravascular tissue in vivo. *J. Exp. Med.* 187:2091–2096.
20. Werr, J., J. Johansson, E.E. Eriksson, P. Hedqvist, E. Ruoslahti, and L. Lindbom. 2000. Integrin $\alpha_2\beta_1$ (VLA-2) is a principal receptor

used by neutrophils for locomotion in extravascular tissue. *Blood*. 95:1804–1809.
21. Bohnsack, J.F. 1992. CD11/CD18-independent neutrophil adherence to laminin is mediated by the integrin VLA-6. *Blood*. 79:1545–1552.
22. Frieser, M., R. Hallmann, S. Johansson, D. Vestweber, S.L. Goodman, and L. Sorokin. 1996. Mouse polymorphonuclear granulocyte binding to extracellular matrix molecules involves β_1 integrins. *Eur. J. Immunol*. 26:3127–3136.
23. Dangerfield, J., K.Y. Larbi, M.T. Huang, A. Dewar, and S. Nourshargh. 2002. CD31 (CD31) homophilic interaction up-regulates $\alpha_6\beta_1$ on transmigrated neutrophils in vivo and plays a functional role in the ability of α6 integrins to mediate leukocyte migration through the perivascular basement membrane. *J. Exp. Med*. 196:1201–1211.
24. Walker, D.C., A.R. Behzad, and F. Chu. 1995. Neutrophil migration through preexisting holes in the basal laminae of alveolar capillaries and epithelium during streptococcal pneumonia. *Microvasc. Res*. 50:397–416.
25. von der Mark, H., I. Oberbaumer, R. Timpl, R. Kemler, and G. Wick. 1985. Immunochemical and autoantigenic properties of the globular domain of basement membrane collagen (type IV). *Eur. J. Biochem*. 146:555–562.
26. Costell, M., E. Gustafsson, A. Aszodi, M. Morgelin, W. Bloch, E. Hunziker, K. Addicks, R. Timpl, and R. Fassler. 1999. Perlecan maintains the integrity of cartilage and some basement membranes. *J. Cell Biol*. 147:1109–1122.
27. Kohfeldt, E., T. Sasaki, W. Gohring, and R. Timpl. 1998. Nidogen-2: a new basement membrane protein with diverse binding properties. *J. Mol. Biol*. 282:99–109.
28. Sorokin, L.M., M. Frieser, S. Kroger, E. Ohage, and R. Deutzmann. 1997. Developmental regulation of the laminin α5 chain suggests a role in epithelial and endothelial cell maturation. *Dev. Biol*. 189:285–300.
29. Sixt, M., B. Engelhardt, F. Pausch, R. Hallmann, O. Wendler, and L.M. Sorokin. 2001. Endothelial cell laminin isoforms, laminin 8 and 10, play decisive roles in T cell recruitment across the blood-brain barrier in experimental autoimmune encephalomyelitis. *J. Cell Biol*. 153:933–945.
30. Newton, R.A., and N. Hogg. 1998. The human S100 protein MRP-14 is a novel activator of the β2 integrin Mac-1 on neutrophils. *J. Immunol*. 160:1427–1435.
31. Burns, A.R., D.C. Walker, E.S. Brown, L.T. Thurmon, R.A. Bowden, C.R. Keese, S.I. Simon, M.L. Entman, and C.W. Smith. 1997. Neutrophil transendothelial migration is independent of tight junctions and occurs preferentially at tricellular corners. *J. Immunol*. 159:2893–2903.
32. Wang, S., J.P. Dangerfield, R.E. Young, and S. Nourshargh. 2005. CD31, α_6 integrins and neutrophil elastase co-operate in mediating neutrophil transmigration. *J. Cell Sci*. 118:2067–2076.
33. Kawabata, K., M. Suzuki, M. Sugitani, K. Imaki, M. Toda, and T. Miyamoto. 1991. ONO-5046, a novel inhibitor of human neutrophil elastase. *Biochem. Biophys. Res. Commun*. 177:814–820.
34. Young, R.E., R.D. Thompson, K. Larbi, M. La, C.E. Roberts, S.D. Shapiro, M. Perretti, and S. Nourshargh. 2004. Neutrophil elastase (NE)-deficient mice demonstrate a non-redundant role for NE in neutrophil migration, generation of pro-inflammatory mediators, and phagocytosis in response to zymosan particles in vivo. *J. Immunol*. 172:4493–4502.
35. Geberhiwot, T., S. Ingerpuu, C. Pedraza, M. Neira, U. Lehto, I. Virtanen, J. Kortesmaa, K. Tryggvason, E. Engvall, and M. Patarroyo. 1999. Blood platelets contain and secrete laminin-8 ($\alpha4\beta1\gamma1$) and adhere to laminin-8 via $\alpha_6\beta_1$ integrin. *Exp. Cell Res*. 253:723–732.
36. Wondimu, Z., T. Geberhiwot, S. Ingerpuu, E. Juronen, X. Xie, L. Lindbom, M. Doi, J. Kortesmaa, J. Thyboll, K. Tryggvason, et al. 2004. An endothelial laminin isoform, laminin 8 ($\alpha4\beta1\gamma1$), is secreted by blood neutrophils, promotes neutrophil migration and extravasation, and protects neutrophils from apoptosis. *Blood*. 104:1859–1866.
37. Sixt, M., R. Hallmann, O. Wendler, K. Scharffetter-Kochanek, and L.M. Sorokin. 2001. Cell adhesion and migration properties of β_2-integrin negative polymorphonuclear granulocytes on defined extracellular matrix molecules. Relevance for leukocyte extravasation. *J. Biol. Chem*. 276:18878–18887.
38. Shapiro, S.D. 2002. Neutrophil elastase. Path clearer, pathogen killer, or just pathologic? *Am. J. Respir. Cell Mol. Biol*. 26:266–268.
39. Cepinskas, G., M. Sandig, and P.R. Kvietys. 1999. PAF-induced elastase-dependent neutrophil transendothelial migration is associated with the mobilisation of elastase to the neutrophil surface and localisation to the migrating front. *J. Cell Sci*. 112:1937–1945.
40. Delacourt, C., S. Herigault, C. Delclaux, A. Poncin, M. Levame, A. Harf, F. Saudubray, and C. Lafuma. 2002. Protection against acute lung injury by intravenous or intratracheal pretreatment with EPI-HNE-4, a new potent neutrophil elastase inhibitor. *Am. J. Respir. Cell Mol. Biol*. 26:290–297.
41. Lee, W.L., and G.P. Downey. 2001. Leukocyte elastase. Physiological functions and role in acute lung injury. *Am. J. Respir. Crit. Care Med*. 164:896–904.
42. Senior, R.M., G.L. Griffin, and R.P. Mecham. 1980. Chemotactic activity of elastin-derived peptides. *J. Clin. Invest*. 66:859–862.
43. Steadman, R., M.H. Irwin, P.L. St John, W.D. Blackburn, L.W. Heck, and D.R. Abrahamson. 1993. Laminin cleavage by activated human neutrophils yields proteolytic fragments with selective migratory properties. *J. Leukoc. Biol*. 53:354–365.
44. Adair-Kirk, T.L., J.J. Atkinson, T.J. Broekelmann, M. Doi, K. Tryggvason, J.H. Miner, R.P. Mecham, and R.M. Senior. 2003. A site on laminin α5, AQARSAASKVKVSMKF, induces inflammatory cell production of matrix metalloproteinase-9 and chemotaxis. *J. Immunol*. 171:398–406.
45. Thompson, R.D., K.E. Noble, K.Y. Larbi, A. Dewar, G.S. Duncan, T.W. Mak, and S. Nourshargh. 2001. Platelet endothelial cell adhesion molecule-1 (CD31)-deficient mice demonstrate a transient and cytokine-specific role for CD31 in leukocyte migration through the perivascular basement membrane. *Blood*. 97:1854–1860.
46. Ringelmann, B., C. Roder, R. Hallmann, M. Maley, M. Davies, M. Grounds, and L.M. Sorokin. 1999. Expression of laminin α1, α2, α4 and α5 chains, fibronectin and tenascin-C in skeletal muscle of dystrophic 129ReJ dy/dy mice. *Exp. Cell Res*. 246:165–182.